Journal of the Nigerian Association of Mathematical Physics
Volume 36, (July, 2016), pp 125 – 134

Analysis of Unsteady Hydromagnetic Boundary Layer Flow in an Inclined Wavy Permeable Wall of a Nanofluid with Soret and Dufour Effects and Heat Generation with Convective Boundary Condition

[1]Yusuf A., [1]Aiyesimi Y.M., [1]Jiya M., [2]Okedayo G. T. and [1]Bolarin G.

[1]Department of Mathematics and Statistics, Federal University of Technology, PMB 65, Minna, 00176-0000 Nigeria, Niger State, Nigeria
[2]Department of Mathematics, Ondo State University of Science and Technology, Okiti-Pupa, Ondo State, Nigeria.

Abstract

Problem of unsteady laminar fluid flow in an inclined parallel permeable walls with the lower wall assumed to be wavy while the upper wall flat in a nanofluid with magnetic field effect, Soret and Dufour effects with convective boundary conditions has been considered. The model is presented in its rectangular coordinate system and incorporates the effects of Brownian motion, and thermophoresis parameter. Similarity solution is presented which depends on the Magnetic parameter (M), Darcy number (Da), Prandtl number (P_r), Lewis number (Le), Brownian motion (N_b), thermophoresis number (N_t), Soret (Sr) number, Dufour (DU) number. It is found that, for the fluid temperature to be relatively low, the heat generation parameter (ϕ_0) has to be kept positive.

Keywords: Adomian Decomposition Method, Nanofluid, Nanopaticles, Thermophoresis,Boundary layer, Channel flow, Soret number, Dufour number.

1.0 Introduction

Among early studies related to the subject of heat transfer from irregular surfaces, is the work of Lekoudis et al. [1] who analyzed the boundary-layer of compressible flows along a corrugated wall. Shankar and Sinha [2] solved the Rayleigh problem along a wavy surface using the perturbation technique. Lessen and Gangwani [3] investigated the effects of low magnitude wall undulations in order to capture the stability of the boundary layer in laminar form. Recently, Rees and Pop [4] studied the effects of stationary plane waves on the natural convection induced by a heated undulated surface in a porous medium numerically. All of the above studies were performed on a single infinitely long horizontal wavy wall configuration without considering the channel-flow argument.

Very recently, Muthuraj and Srinivas [5] studied the combined free and force convection considering both heat and mass transfer within a vertical corrugated porous channel with traveling thermal waves. Using the perturbation technique, the effects of different pertinent parameters, namely, the Hartmann number, Schmidt number, and the porosity parameter, on the flow fields and heat and mass transfer characteristics were explained. Umavathi and Shekar [6] investigated the combined convection fluid flow and heat transfer through a long vertical corrugated channel filled with porous material, employing linearization technique. They assumed long wave approximation for perturbation solution. Gireesha and Mahanthesh [7] conducted an analytical approach for combined heat and mass transfer of an unsteady magnetohydrodynamics viscoelastic fluid flow in an irregular vertical channel with coupled boundary condition using perturbation technique. They analyzed the effects of different pertinent parameters such as Sherwood number and Biot number on velocity and temperature fields. Kumar and Umavathi [8] conducted the perturbation technique to problem of steady two-dimensional natural convective flow in a porous medium between a long vertical undulated wall and parallel flat wall in the presence of a heat source utilizing a Walters fluid (model B′). They discussed the relevant flow and heat transfer

Corresponding author: Yusuf A., E-mail: yusuf.abdulhakeem@futminna.edu.ng, Tel.: +2347032143075

characteristics, namely, skin friction and the rate of heat transfer at both walls, in detail. Umavathi and Shekar [9] conducted the same method to laminar mixed convection in a wavy-vertical channel filled with two unmixable viscous fluids. They found that the Grashof number, viscosity parameter, geometry ratio and conductivity ratio enhance the velocity component parallel to the flow direction.

Sheikholeslami et al. [10] studied the magnetic field effect on CuO–water nanofluid flow and heat transfer in an enclosure which is heated from below. They found that effect of Hartmann number and heat source length is more pronounced at high Rayleigh number. Effect of nanofluid on heat transfer enhancement has been investigated by different authors [11]. Aiyesimi et al [12] considers Hydromagnetic Boudary-Layer Flow of a Nanofluid Past a Stretching Sheet Embedded in a Darcian Porous Medium with Radiation and it was found out that at lower values of Prandtl number, heat able to diffused more rapidly out of the system.

In a recent paper Aiyesimi et al[13] extended the model of Khan and Pop [14]to analyse andinvestigate the convective boundary-layer flow of a nanofluid past a stretching sheet with radiation.It was observed that both thermal bouyancy and nanofraction bouyancy enhaces the fluid veloctity, temperure, and nanofraction. It is appropriate to channelize the work of Aiyesimi et al[12] over an inclined permeable wavy channel with magnetic field, Soret and Duffour effectsand use the Adomian Decompositon Method (ADM) to obtain the analytical solution of the model.

This work is a new development in the literature in which an analytical solution of a nanofluid in an inclined permeable wavy channel with Soret and Duffour effects is proposed using the Adomian Decomposition Method.

2.0 Problem Formulation

Consider unsteady, two dimensional boundary layer flow of a nanofluid in an inclined porous, permeable channel at angle Θ. It is assumed that a wavy wall is located at $y = a\cos(\mathrm{Lx})$ while the other flat wall is located at a variable distance $y = h(\mathrm{t}) = \sqrt{\dfrac{\upsilon(1-\lambda\,\mathrm{t})}{a}}$ (h= is the width of the channel) and a is the amplitude of the wavy wall and Lx is a location on the wavy wall. The temperature T has no constant value at the wavy wall while nanoparticle fraction C have constants value C_0 at $y = aCos(\mathrm{Lx})$ and T_h and C_h at $y = h(\mathrm{t})$ respectively. For this application, we will adopt the formulation of Aiyesimi[12] in a porous wavy wall with permeability, magnetic field, Soret, Dufour, Heat generation effects with convective boundary conditions, and it is governed by the following equations:

Continuity equation:-

$$\frac{\partial u}{\partial x}+\frac{\partial v}{\partial y}=0 \tag{1}$$

Momentum equation:

$$\frac{\partial u}{\partial t}+u\frac{\partial u}{\partial x}+v\frac{\partial u}{\partial y}=-\frac{1}{\rho_f}\frac{\partial p}{\partial x}+\upsilon\left(\frac{\partial^2 u}{\partial x^2}+\frac{\partial^2 u}{\partial y^2}\right)-\frac{\upsilon\varphi}{k}u-c\varphi u^2-\frac{\sigma B_0^{\,2}}{\rho}u$$
$$+g\beta(T-T_h)\cos\Theta+g\beta(C-C_h)\cos\Theta \tag{2}$$

Energy equation:-

$$\frac{\partial T}{\partial t}+u\frac{\partial T}{\partial x}+v\frac{\partial T}{\partial y}=\alpha\left(\frac{\partial^2 T}{\partial x^2}+\frac{\partial^2 T}{\partial y^2}\right)+\frac{Q}{\rho c_p}(T-T_h)$$
$$+\tau\left(D_B\left(\frac{\partial C}{\partial x}\frac{\partial T}{\partial x}+\frac{\partial C}{\partial y}\frac{\partial T}{\partial y}\right)+\frac{D_T}{T_h}\left(\left(\frac{\partial T}{\partial x}\right)^2+\left(\frac{\partial T}{\partial y}\right)^2\right)\right)+\frac{D_M K_T}{C_S C_p}\frac{\partial^2 C}{\partial y^2} \tag{4}$$

Nanofraction equation:-

$$\frac{\partial C}{\partial t}+u\frac{\partial C}{\partial x}+v\frac{\partial C}{\partial y}=D_B\left(\frac{\partial^2 C}{\partial x^2}+\frac{\partial^2 C}{\partial y^2}\right)+\left(\frac{D_M K_T}{T_M}\right)\left(\frac{\partial^2 T}{\partial y^2}+\frac{\partial^2 T}{\partial y^2}\right) \tag{5}$$

Subject to the boundary conditions:

$$y = aCos(\mathrm{Lx}): u = 0, \qquad v = v_0, \qquad -k^*\frac{\partial T}{\partial y} = h^*(T_f - T_h), \qquad C = C_0$$

$h(t): u \to 0, T \to T_h, C \to C_0, (6)$

Where u and v are the velocity components along the x and y axes respectively, p is the fluid pressure, ρ_f is the density of the base fluid, t is the time, α is the thermal diffusivity, υ is the kinematic viscousity, k^* is the thermal conductivity, k is the permeability, σ is the electrical conductivity, K_T is the thermal-diffusion ratio, T_f is the convective fluid temperature, h^* is the convective heat transfer coefficient, φ is the porousity, B_0 external magnetic field, Q is the heat generation, C_p is the specific heat capacity at constant pressure, D_B is the Brownian diffusion coefficient, D_T is the thermopheric diffusion coefficient and $\tau = \dfrac{(\rho c)_p}{(\rho c)_f}$ is the ratio between the effective heat capacity of the fluid with ρ being the density, c is Forchheimer's inertia coefficient and ρ_p is the density of the particles, g is the acceleration due to gravity, T_M is the mean fluid temperature, C_S is concentration susceptibility.

Defining the dimensional stream function $\left(\psi(x,y)\right)$ in the usual way such that $u = \dfrac{\partial \psi}{\partial y}$ and $v = -\dfrac{\partial \psi}{\partial x}$ and following the work in [10] :-

$$\eta = \frac{y}{h(t)}, \psi = x\sqrt{\frac{a\upsilon}{1-\lambda t}} f(\eta), \theta(\eta) = \frac{T - T_h}{T_0 - T_h}, \text{ and } \chi(\eta) = \frac{C - C_h}{C_0 - C_h} \quad (7)$$

where η, $f(\eta)$, $\theta(\eta)$, $\chi(\eta)$ are the dimensionless fluid distance, velocity profile, temperature profile, and nanoparticle concentration.

Neglecting the pressure gradient, equations (1) to (6) reduces to the following local similaritysolution:-

$$f''' - \frac{A}{2}\eta f'' + ff'' - (1+\phi) f'^2 - \mathrm{Re}\left(Da^{-1} + M\right) f' + Cos\Theta\left(G_{rT}\theta + G_{rC}\chi\right) = 0 \quad (8)$$

$$\theta'' - \frac{A}{2}\eta\theta' + \mathrm{Pr} f\theta' + \mathrm{Re}\,\mathrm{Pr}\,\phi_0\theta + \mathrm{Pr}\,N_b\chi'\theta' + \mathrm{Pr}\,N_t\theta'^2 + \mathrm{Pr}\,DU\chi'' = 0 \quad (9)$$

$$\chi'' - \frac{A}{2}\eta\chi' + \mathrm{Re}\,Lef\chi' + LeS_r\theta'' = 0 \quad (10)$$

with corresponding boundary conditions:

$$f(0) = f_0,\ f'(0) = 0,\ \theta'(0) = -B_i\left(1 - \theta(0)\right),\ \chi(0) = 1,$$
$$f'(1) = 0,\ \theta(1) = 0,\ \chi(1) = 0. \quad (11)$$

in which : $f_0 = -v_0\sqrt{\dfrac{(1-\lambda t)}{a\upsilon}}$, $Gr_{Tx} = \dfrac{g_0\beta(T_0 - T_h)}{\upsilon^2}$, $Gr_{Cx} = \dfrac{g_0\beta(C_0 - C_h)}{\upsilon^2}$, $A = \dfrac{\lambda}{a}$, $\phi = c\varphi$, $Da^{-1} = \dfrac{\upsilon\varphi}{ak}$,

$\mathrm{Re} = \dfrac{h(t)}{\upsilon}$ $M = \dfrac{\sigma B_0^{\,2}}{a\rho}$, $P_r = \dfrac{\upsilon}{\alpha}$, $Le = \dfrac{\upsilon}{D_B}$, $\phi_0 = \dfrac{hQ}{\upsilon\rho C_p}$, $B_i = \dfrac{h^*}{k^*}\left(\dfrac{\upsilon(1-\lambda t)}{a}\right)^{1/2}$, $N_b = \dfrac{(\rho c)_p D_B (C_0 - C_h)}{(\rho c)_f \upsilon}$,

$N_t = \dfrac{(\rho c)_p D_T (T_0 - T_h)}{(\rho c)_f T_h \upsilon}$, $DU = \dfrac{D_M K_T (C_0 - C_h)}{C_S C_p (T_0 - T_h)}$, $S_r = \dfrac{D_M K_T (T_0 - T_h)}{T_M \upsilon (C_0 - C_h)}$. are the Suction parameter, Thermal Grashof number, modified Grashof number, unsteady parameter, inertia coefficient, inverse Darcy number, Renold number, Magnetic Parameter, Prandtl number, Lewis number, heat generation or absorption parameter, Biot number, Brownian motion parameter, thermophoresis parameter, Dufour number, and Soret number respectively.

Table 1: Comparison of Result for $\theta(\eta)$ with the present work for $P_r = 1$, $Da^{-1} = 0$, $M=0$, $DU = 0$ and $Gr_c = 0$, $A = 0.1$, $Le = 1$

η	RK-Method	Present Work
0.0	0.9999	1.0000
0.1	0.8899	0.8726
0.2	0.7803	0.7641
0.3	0.6721	0.6565
0.4	0.5661	0.5512
0.5	0.4628	0.4491
0.6	0.3629	0.3507
0.7	0.2665	0.2566
0.8	0.1738	0.1668
0.9	0.08504	0.0813
1	0.0000	0.0000

3.0 Results and Discussion

The nonlinear coupled differential equations (8) to (10) with boundary conditions (11) are solved using the Modfied Adomian Decomposition Methods by Ebaid and Al-armani [15]. In order to assess the accuracy of the present method, we have compared our solution for $\theta(\eta)$ for different values of η with the Numerical method with $\theta'(0) = 0$ as shown in Table 1. It was observed that the present method is in good agreement with the Numerical method.

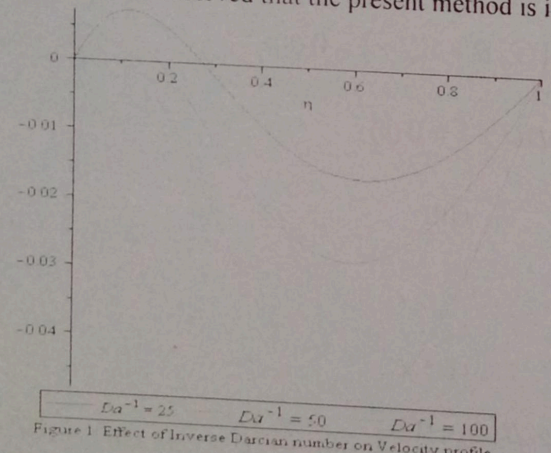

Figure 1 Effect of Inverse Darcian number on Velocity profile

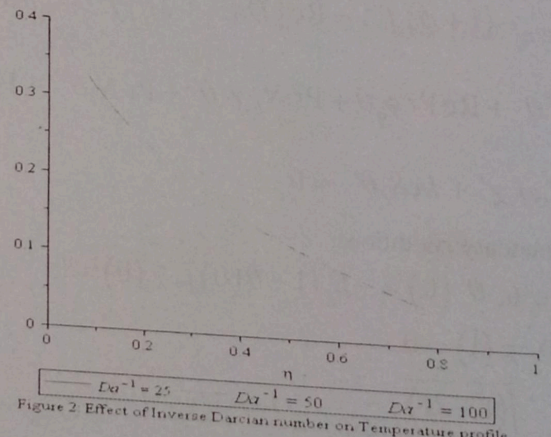

Figure 2 Effect of Inverse Darcian number on Temperature profile

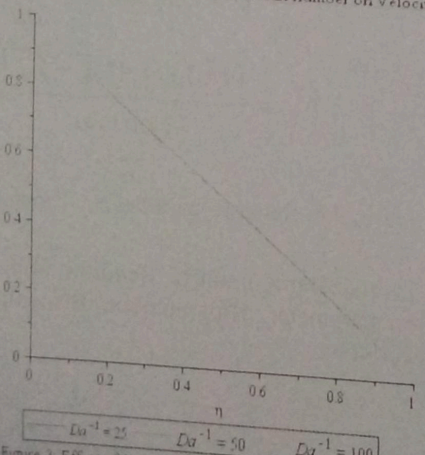

Figure 3 Effect of Inverse Darcian number on Nanofraction profile

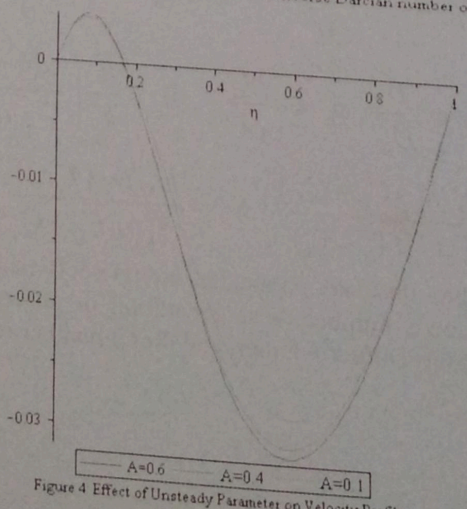

Figure 4 Effect of Unsteady Parameter on Velocity Profile

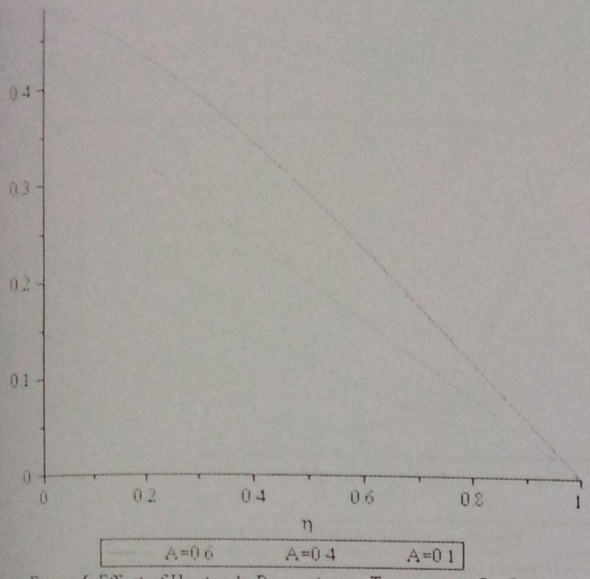

Figure 5: Effect of Unsteady Parameter on Temperature Profile

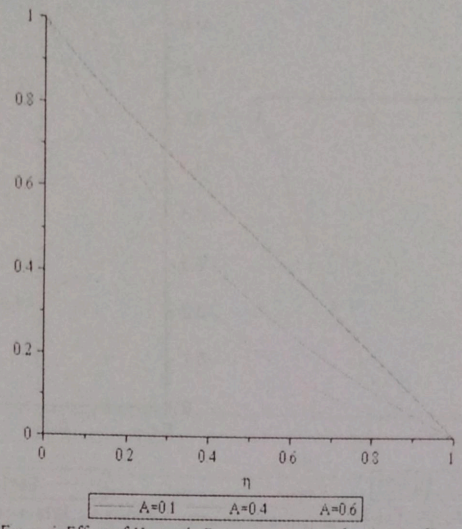

Figure 6: Effect of Unsteady Parameter on Nanofraction Profile

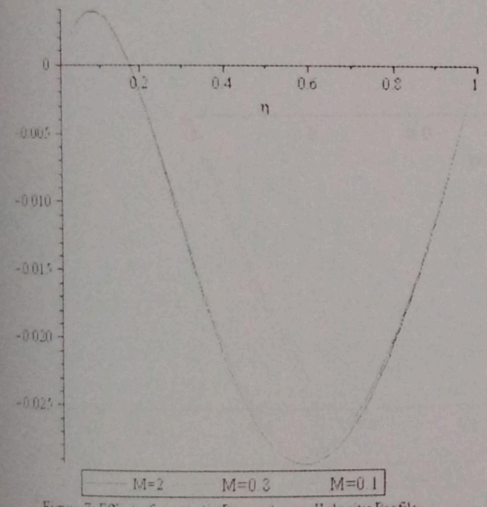

Figure 7: Effect of magnetic Parameter on Velocity Profile

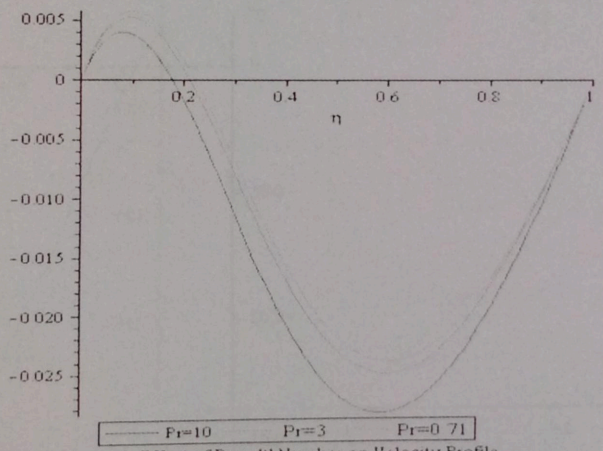

Figure 8: Effect of Prandtl Number on Velocity Profile

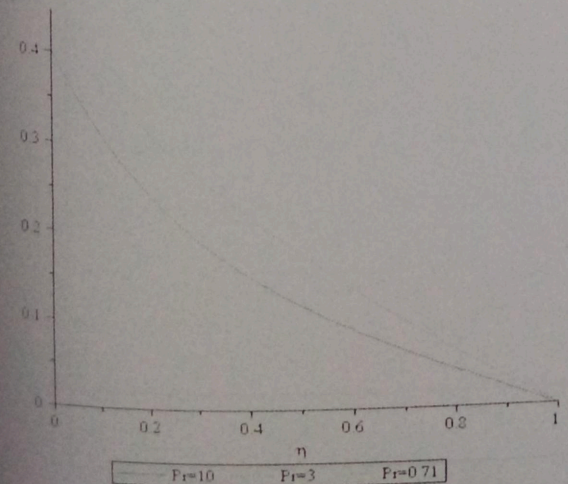

Figure 9: Effect of Prandtl Number on Temperature Profile

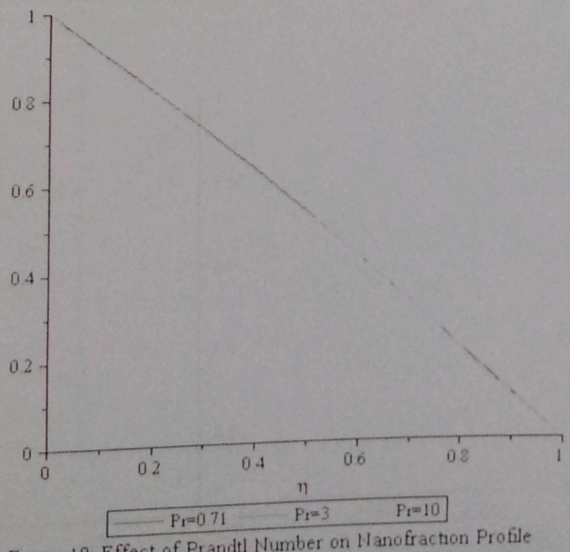

Figure 10: Effect of Prandtl Number on Nanofraction Profile

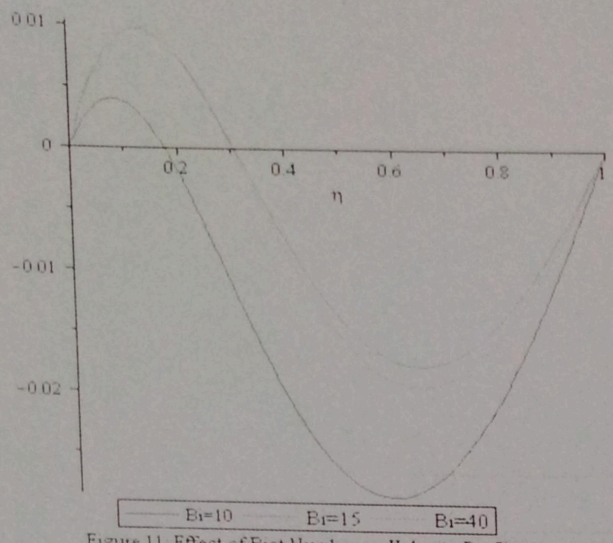

Figure 11: Effect of Biot Number on Velocity Profile

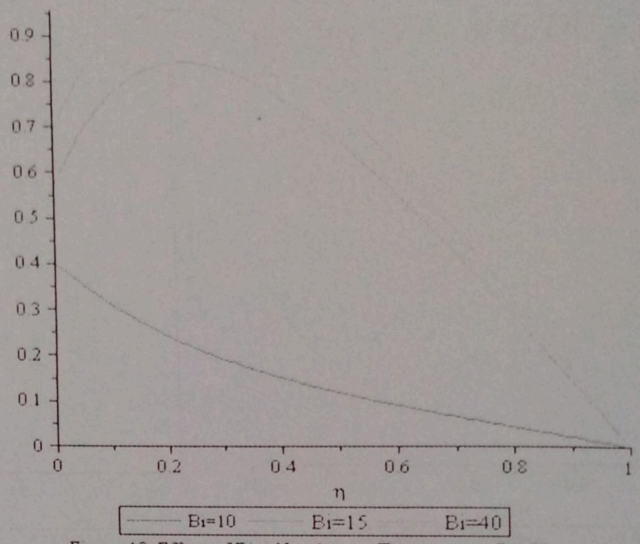

Figure 12: Effect of Biot Number on Temperature Profile

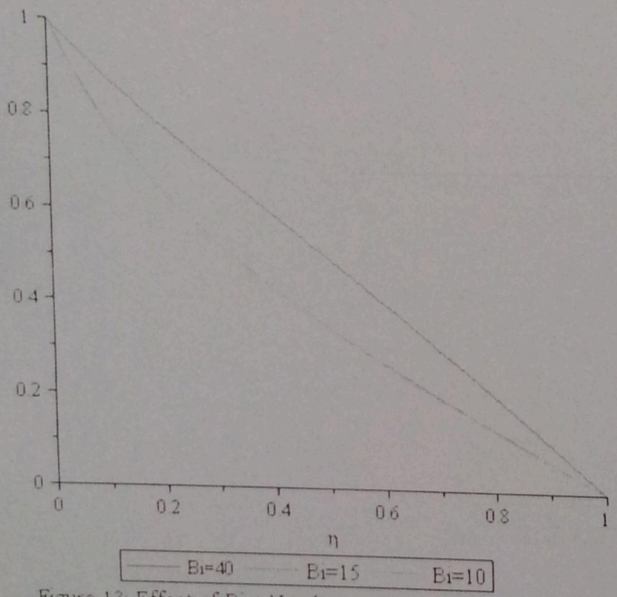

Figure 13: Effect of Biot Number on Nanofraction Profile

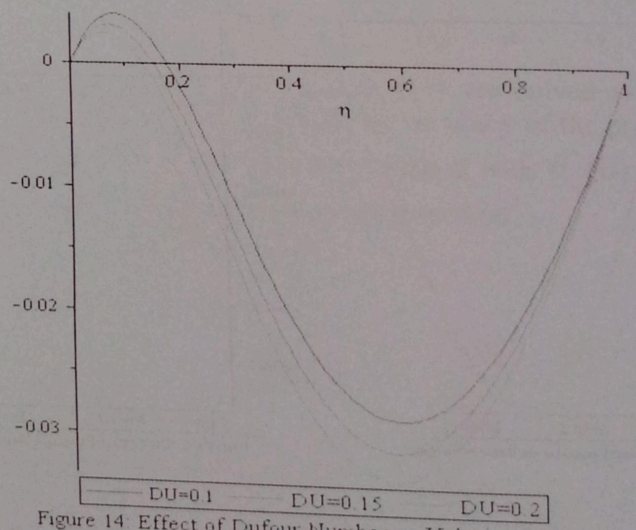

Figure 14: Effect of Dufour Number on Velocity Profile

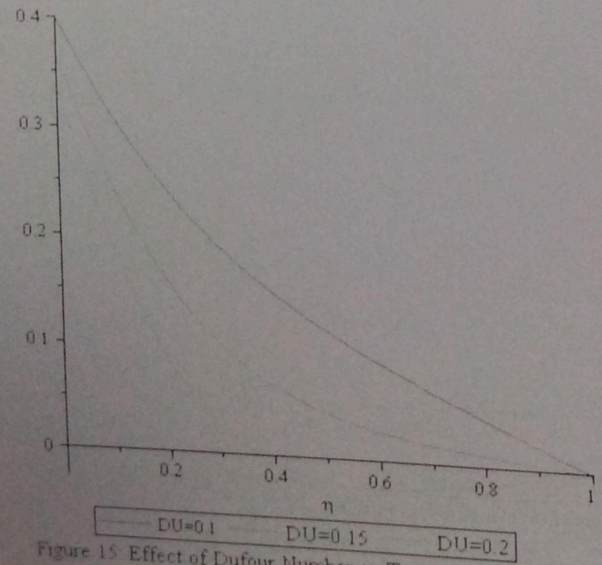

Figure 15: Effect of Dufour Number on Temperature Profile

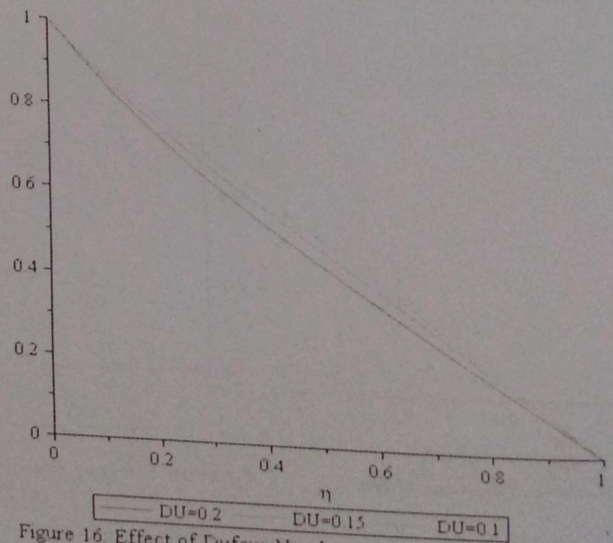

Figure 16: Effect of Dufour Number on Nanofraction Profile

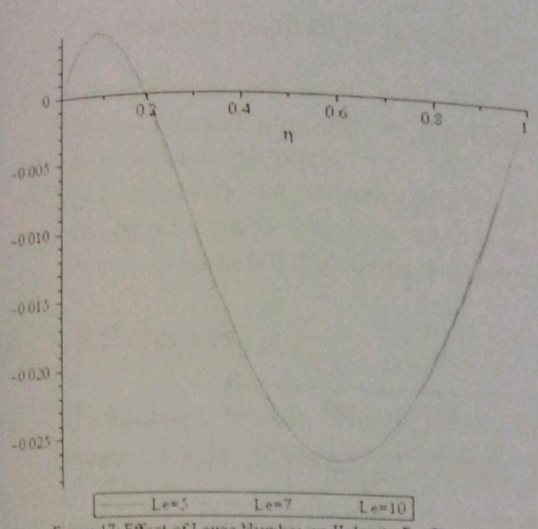

Figure 17: Effect of Lewis Number on Velocity Profile

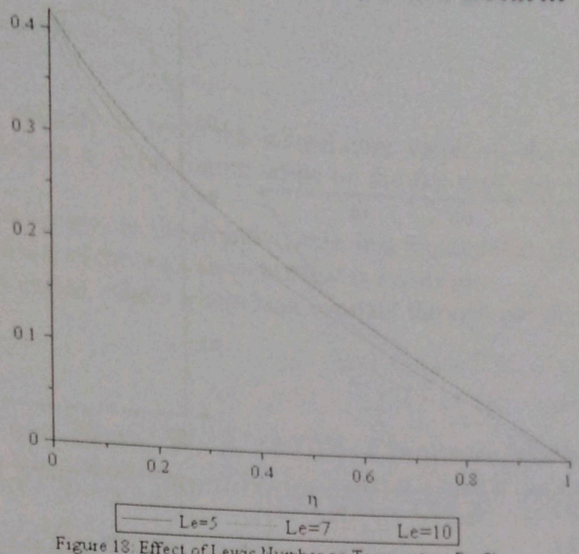

Figure 18: Effect of Lewis Number on Temperature Profile

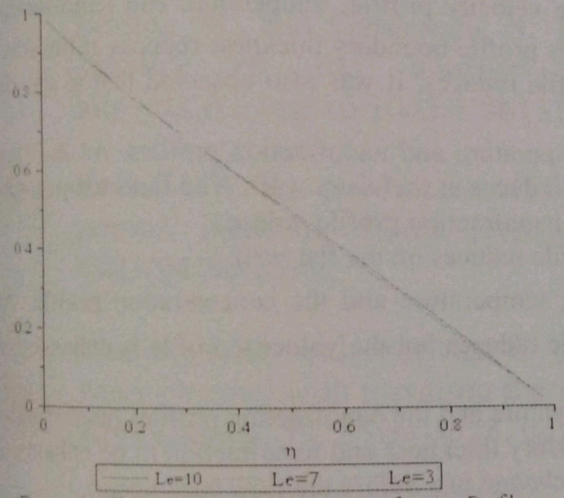

Figure 19: Effect of Lewis Number on Nanofraction Profile

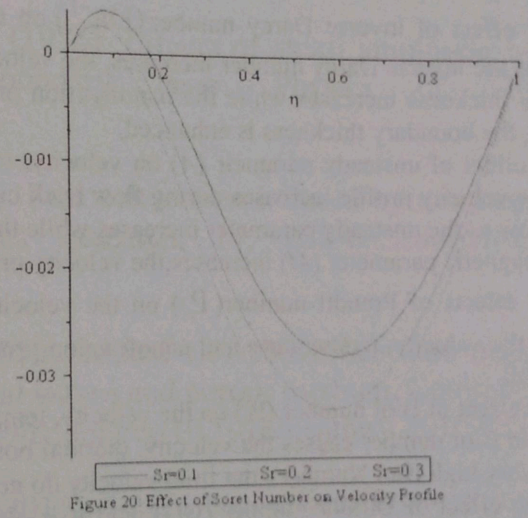

Figure 20: Effect of Soret Number on Velocity Profile

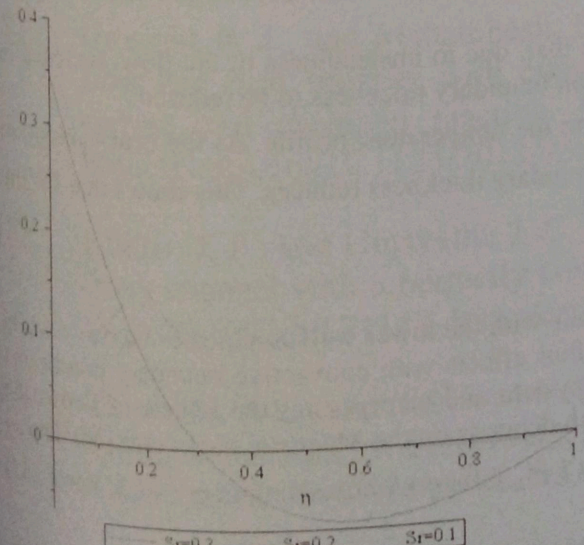

Figure 21: Effect of Soret Number on Temeperature Profile

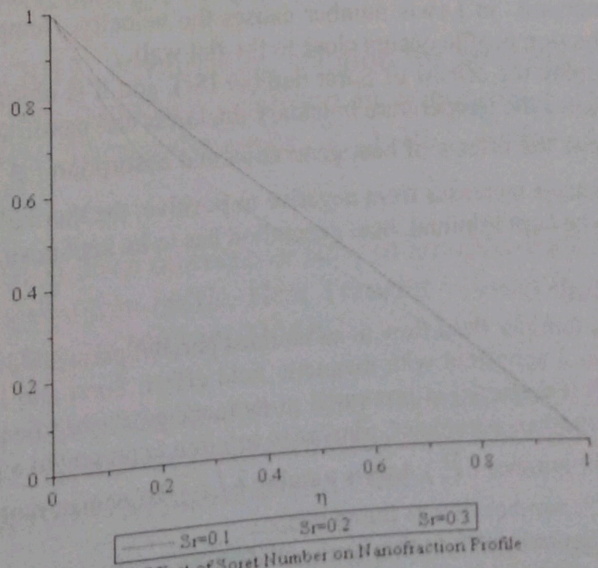

Figure 22: Effect of Soret Number on Nanofraction Profile

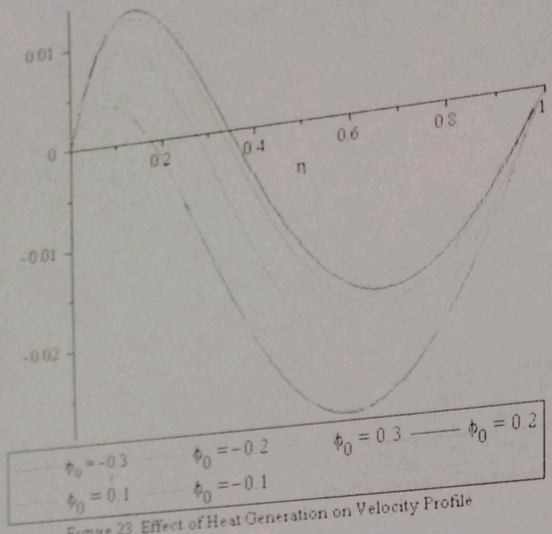

Figure 23 Effect of Heat Generation on Velocity Profile

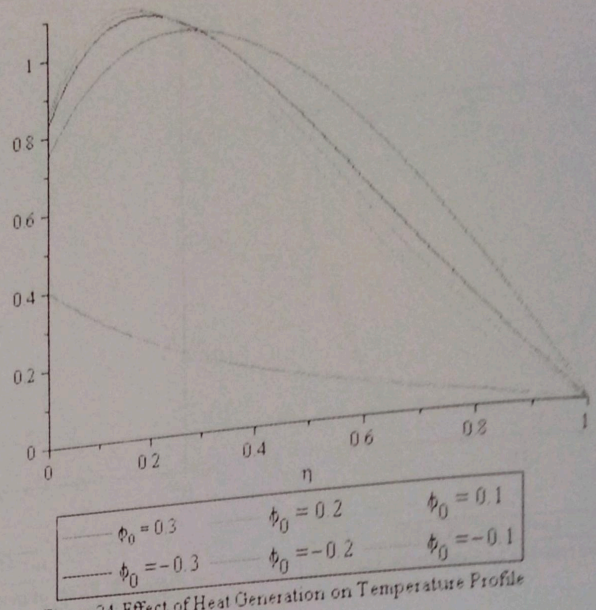

Figure 24 Effect of Heat Generation on Temperature Profile

Figures 1 to 3 present the effect of inverse Darcy number (Da^{-1}) on the velocity profile, temperature and nanofraction profile. It is observed that as the inverse Darcy number increases, the velocity profile boundary thickness reduces at the wavy wall, and thermal boundary thickness increases while the nanofraction profile reduces. It was also observed that at the flat wall, as the fluid flow back, the boundary thickness is enhanced.

Figures 4 to 6 display the effect of unsteady parametr (A) on velocity, temperature and nanofraction profiles. As the flow becomes more unsteady, the velocity profile increases during flow back but reduces at the wavy wall. The fluid temperature increases through out the flow as the unsteady parameter increases while the nanofraction profile reduces.

Figure 7 shows that as themagnetic parameter (M) increases,the velocity profile reduces on the flat wall.

Figures 8 to 10 depict the effects of Prandtl number(P_r) on the velocity, temperature and the concentration profile. As Prandtle number increases, the velocity, temperature and nanofraction profile reduces but the velocity profile is enhanced at the middle of the parallel wall.

Figures 11 to 13 present the effect of Biot number ($\mathrm{B_i}$) on the velocity, temperature and the nanofraction profiles respectively. It is observed that increase in Biot number causes the velocity, thermal boundary thickness and nanofraction to be enhanced. It is also observed that at a very high Biot Number , the fluid velocity do not change just before the flow back occur.

Figures 14 to 16 display the effect of Dufour number (DU), and it is observe that, increase in Dufour number causes the velocity, temperature boundary thickness and nanofraction boundary thickness to reduced.

Figures 17 to 19 present the effect of Lewis number (Le) on velocity, temperature and the nanofraction profiles respectively. It is observe that increase in Lewis number causes the velocity, temperature profile and nanofraction profiles to reduce. Reduction in nanofraction profile occurs close to the flat wall.

Figures 20 to 22 display the effects of Soret number (Sr), and it is observe that, due to unsteadiness of the flow, increase in the Soret number causes the temperature boundary thickness and nanofraction boundary thickness to be reduced.

Figures 23 to 24 show the effects of heat generation and absorption (ϕ_0) on the temperature profile. As the heat generation and absorption parameter increases from negative to positive, the thermal boundary thickness reduces. This shows that for the fluid temperature to be kept minimal, heat generation has to be kept positive.

4.0 Conclusion

Problem of unsteady laminar fluid flow in an inclined parallel permeable walls with the lower wall assumed to be wavy while the upper wall flat in a nanofluid with magnetic field effect, Soret and Dufour effects with convective boundary condition has been considered. The model is presented in its rectangular coordinate system and incorporates the effects of Brownian motion, and thermophoresis parameter. Similarity solution is presented which depends on the Magnetic parameter (M), Darcy number (Da), Prandtl number (P_r), Lewis number (Le), Brownian motion (N_b), thermophoresis number (N_t), Soret number, Dufour (DU) number. It was found that:-

1. All the graphs presented in this work satisfy the boundary conditions.
2. The results obtained in this work are in good agreement with the Numerical Methods as shown in Table 1 which proves the efficiency of the method.

3. The problem is solved by taking $Lx = \frac{\pi}{2}$.

4. Generally on the wavy wall, the fluid velocity is zero, the temperature varies as the parameter as a result of convective heating, and the fluid nanofraction is at maximum while on the flat wall, the velocity, temperature and nanofraction are zeros.

5. It is observed that, velocity profile graphs crosses to the negative axis, this implies that, there is a flow back within the parallel walls. The flow back is as a result of the wall waviness that is involved.

6. It should be noted that while a quantity is varied, others where kept constant through out the work.

5.0 References

[1] Lekoudis, S. G., Nayfeh, A. H., and Saric, W. S. (1976). Compressible boundary layers over wavy walls. Physics of Fluids, 19, 514–519. http://dx.doi.org/10.1063/1.861507.

[2] Shankar, P. N., and Sinha, U. N. (1976). The Rayleigh problem for a wavy wall. Journal of Fluid Mechanics, 77, 243–256. http://dx.doi.org/10.1017/S0022112076002097.

[3] Lessen, M., and Gangwani, S. T. (1976). Effects of small amplitude wall waviness upon the stability of the laminar boundary layer. Physics of Fluids, 19, 510–513. http://dx.doi.org/10.1063/1.861515.

[4] Rees, D. A. S., and Pop, I. (1994). Free convection induced by a horizontal wavy surface in a porous medium. Fluid Dynamics Research, 14, 151–66. http://dx.doi.org/10.1016/0169-5983(94)90026-4.

[5] Muthuraj, R., and Srinivas, S. (2010). Mixed convective heat and mass transfer in a vertical wavy channel with traveling thermal waves and porous medium. Computers & Mathematics with Applications, 59, 3516–3528. http://dx.doi.org/10.1016/j.camwa.2010.03.045.

[6] Umavathi, J. C., and Shekar, M. (2011). Mixed convection flow and heat transfer in a vertical wavy channel containing porous and fluid layer with traveling thermal waves. International Journal of Engineering, Science and Technology, 197(3), 196-219.

[7] Gireesha B. J., and Mahanthesh, B. (2013). Perturbation solution for radiating viscoelastic fluid flow and heat transfer with convective boundary condition in nonuniform channel with hall current and chemical reaction. ISRN Thermodynamics, 2, 1-16. Article ID 935481, 14. http://dx.doi.org/10.1155/2013/935481.

[8] Kumar, J. P., and Umavathi, J. C. (2013). Free convective flow in an open-ended vertical porous wavy channel with a perfectly conductive thin baffle. Heat Transfer—Asian Research, 3, 46-58. DOI: 10.1002/htj.21118. http://dx.doi.org/10.1002/htj.21118.

[9] Umavathi, J. C., and Shekar, M. (2014). Mixed convective flow of immiscible fluids in a vertical corrugated channel with traveling thermal waves. Journal of King Saud University – Engineering Sciences, 26, 49–68. http://dx.doi.org/10.1016/j.jksues.2012.11.002.

[10] M. Sheikholeslami, M. Gorji-Bandpy, R. Ellahi, A. Zeeshan (2014). Simulation of MHD CuO–water nanofluid flow and convective heat transfer considering Lorentz forces, J. Mag. Magn. Mater. 369, 69–80.

[11] A.Sh. Kherbeet, H.A. Mohammed, B.H. Salman (2012). The effect of nanofluids flow on mixed convection heat transfer over microscale backward-facing step, Int. J. Heat Mass Transfer 55, 5870–5881.

[12] Aiyesimi, Y.M., Yusuf, A. and Jiya, M. (2015). Hydromagnetic Boudary-Layer Flow of a Nanofluid Past a Stretching Sheet Embedded in a Darcian Porous Medium with Radiation. Nigerian Journal of Mathematics and Applications, 24, 13-29.

[13] Aiyesimi, Y.M. Yusuf, A. and Jiya, M. (2015). An Analytic Investigation Of Convective Boundary-Layer Flow Of A Nanofluid Past A Stretching Sheet With Radiation. Journal of Nigerian Association of Mathematical Physics. 29 (1), 477-490.

[14] Khan, W.A., Pop, I.(2010). Boundary-layer flow of a nanofluid past a stretching sheet, Int. J. Heat Mass Transf. 53, 2477-2483 (2010).

[15] Ebaid, A. and Al-Armani, N. (2013). An Approach for a Class of the Blasius Problem via a Transformation and Adomian's Method. Abstract and Applied Analysis, the Scientific World Journal.